
Few-Shot One-Class Classification via Meta-Learning

Ahmed Frikha

Siemens AG, Corporate Technology
Ludwig Maximilian University of Munich
Munich, Germany
ahmed.frikha@siemens.com

Denis Krompaß

Siemens AG, Corporate Technology
Munich, Germany

Hans-Georg Köpken

Siemens AG, Corporate Technology
Munich, Germany

Volker Tresp

Siemens AG, Corporate Technology
Ludwig Maximilian University of Munich
Munich, Germany

Abstract

Although few-shot learning and one-class classification (OCC), i.e. learning a binary classifier with data from only one class, have been separately well studied, their intersection remains rather unexplored. Our work addresses the few-shot OCC problem and presents a method to modify the episodic data sampling strategy of the model-agnostic meta-learning (MAML) algorithm to learn a model initialization particularly suited for learning few-shot OCC tasks. This is done by explicitly optimizing for an initialization which only requires few gradient steps with one-class minibatches to yield a performance increase on class-balanced test data. We provide a theoretical analysis that explains why our approach works in the few-shot OCC scenario, while other meta-learning algorithms, including MAML, fail. Our experiments on eight datasets from the image and time-series domains show that our method leads to higher results than classical OCC and few-shot classification approaches, and demonstrate the ability to learn unseen tasks from only few normal class samples. Moreover, we successfully train anomaly detectors for a real-world application on sensor readings recorded during industrial manufacturing of workpieces with a CNC milling machine using few normal examples. Finally, we empirically demonstrate that the proposed data sampling technique increases the performance of more recent meta-learning algorithms in few-shot OCC.

1 Introduction

The anomaly detection (AD) task [7, 1] consists in differentiating between normal and abnormal data samples. AD applications are common in various domains that involve different data types, including medical diagnosis [34], cybersecurity [12] and quality control in industrial manufacturing [46]. Due to the rarity of anomalies, the data underlying AD problems exhibits high class-imbalance. Therefore, AD problems are usually formulated as one-class classification (OCC) problems [31], where either only a few or no anomalous data samples are available for training the model [19]. While most of the developed approaches [19] require a substantial amount of normal data to yield good generalization, in many real-world applications, e.g. in industrial manufacturing, only small datasets are available. Data scarcity can have many reasons: data collection itself might be expensive, e.g. in healthcare, or happens only gradually, such as in a cold-start situation, or the domain expertise required for annotation is scarce and expensive.

To enable learning from few examples, viable approaches [24, 37, 10] relying on meta-learning [43] have been developed. However, they rely on having examples from each of the task’s classes, which

prevents their application to OCC tasks. While recent meta-learning approaches focused on the few-shot learning problem, i.e. learning to learn with few examples, we extend their use to the OCC problem, i.e. learning to learn with examples from only one class. To the best of our knowledge, the few-shot OCC (FS-OCC) problem has only been addressed in [22, 23] in the image domain.

Our contribution is fourfold: Firstly, we show that classical OCC approaches fail in the few-shot data regime. Secondly, we provide a theoretical analysis showing that classical gradient-based meta-learning algorithms do not yield parameter initializations suitable for OCC tasks and that second-order derivatives are needed to optimize for such initializations. Thirdly, we propose an episode generation strategy to adapt the model-agnostic meta-learning (MAML) algorithm [10] to learn initializations useful for the FS-OCC scenario. The resulting One-Class MAML (OC-MAML) maximizes the inner product of loss gradients computed on one-class and class-balanced minibatches, hence maximizing the cosine similarity between these gradients. Finally, we demonstrate that the proposed data sampling technique generalizes beyond MAML to other metalearning algorithms, e.g. MetaOptNet [27] and Meta-SGD [29], by successfully adapting them to the understudied FS-OCC problem.

We empirically validate our approach on eight datasets from the image and time-series domains, and demonstrate its robustness and maturity for real-world applications by successfully testing it on a real-world dataset of sensor readings recorded during manufacturing of metal workpieces with a CNC milling machine.

2 Approach

The primary contribution of our work is to propose a way to adapt meta-learning algorithms designed for class-balanced FS learning to the underexplored FS-OCC problem. In this section, as a first demonstration that meta-learning is a viable approach to this challenging learning scenario, we focus on investigating it on the MAML algorithm. MAML was shown to be a universal learning algorithm approximator [11], i.e. it could approximate a learning algorithm tailored for FS-OCC. Later, we validate our methods on further meta-learning algorithms (Table 3).

2.1 Problem statement

Our goal is to learn a one-class classification (OCC) task using only a *few* examples. In the following, we first discuss the unique challenges of the few-shot one-class classification (FS-OCC) problem. Subsequently, we discuss the formulation of the FS-OCC problem as a meta-learning problem.

To perform one-class classification, i.e. differentiate between in-class and out-of-class examples using only in-class data, approximating a *generalized* decision boundary for the normal class is necessary. Learning such a class decision boundary in the few-shot regime can be especially challenging for the following reasons. On the one hand, if the model overfits to the few available datapoints, the class decision boundary would be too restrictive, which would prevent generalization to unseen examples. As a result, some normal samples would be predicted as anomalies. On the other hand, if the model overfits to the majority class, i.e. predicting almost everything as normal, the class decision boundary would overgeneralize, and out-of-class (anomalous) examples would not be detected.

In the FS classification context, N -way K -shot learning tasks are used to test the learning procedure yielded by the meta-learning algorithm. An N -way K -shot classification task includes K examples from *each* of the N classes that are used for learning this task, after which the trained classifier is tested on a disjoint set of data [52]. When the target task is an OCC task, only examples from one class are available for training, which can be viewed as a 1-way K -shot classification task. To align with the anomaly detection problem, the available examples must belong to the normal (majority) class, which usually has a lower variance than the anomalous (minority) class. This problem formulation is a prototype for a practical use case where an application-specific anomaly detector is needed and only few normal examples are available.

2.2 Model-Agnostic Meta-Learning

MAML is a meta-learning algorithm that we focus on adapting to the FS-OCC problem. MAML learns a model initialization that enables quick adaptation to unseen tasks using only few data samples.

For that, it trains a model explicitly for few-shot learning on tasks T_i coming from the same task distribution $p(T)$ as the unseen target task T_{test} . In order to assess the model’s adaptation ability to *unseen* tasks, the available tasks are divided into mutually disjoint task sets: one for meta-training S^{tr} , one for meta-validation S^{val} and one for meta-testing S^{test} . Each task T_i is divided into two disjoint sets of data, each of which is used for a particular MAML operation: D^{tr} is used for adaptation and D^{val} is used for validation, i.e. evaluating the adaptation. The adaptation of a model f_θ to a task T_i consists in taking few gradient descent steps using *few* datapoints sampled from D^{tr} yielding θ'_i .

A good measure for the suitability of the initialization parameters θ for few-shot adaptation to a considered task T_i is the loss $L_{T_i}^{val}(f_{\theta'_i})$, which is computed on the validation set D_i^{val} using the task-specific adapted model $f_{\theta'_i}$. In order to optimize for few-shot learning, the model parameters θ are updated by minimizing the aforementioned loss across all meta-training tasks. This update, called the *meta-update*, can be expressed as:

$$\theta \leftarrow \theta - \beta \nabla_\theta \sum_{T_i \sim p(T)} L_{T_i}^{val}(f_{\theta'_i}). \quad (1)$$

Here β is the learning rate used for the meta-update. To avoid overfitting to the meta-training tasks, model selection is done via validation using tasks from S^{val} . At meta-test time, the FS adaptation to unseen tasks from S^{test} is evaluated. We note that, in the case of few-shot classification, K datapoints from *each* class are sampled from D^{tr} for the adaptation, during training and testing.

2.3 One-Class Model-Agnostic Meta-Learning

2.3.1 Algorithm

MAML learns a model initialization suitable for *class-balanced* (CB) FS classification. To adapt it to FS-OCC, our motivation consists in finding a model initialization from which taking few gradients steps with a few one-class (OC) examples yields the same effect as doing so with a CB minibatch. We achieve this by adequately modifying the objective of the inner loop updates of MAML. Concretely, this is done by modifying the data sampling technique during meta-training, so that the class-imbalance rate (CIR) of the inner loop minibatches matches the one of the test task.

MAML optimizes explicitly for FS adaptation by creating and using auxiliary tasks that have the same characteristic as the target tasks, in this case tasks that include only few datapoints for training. It does so by reducing the size of the batch used for the adaptation (via the hyperparameter K [11]). Analogously, OC-MAML trains explicitly for quick adaptation to OCC tasks by creating OCC auxiliary tasks for meta-training. As described in Section 1, OCC problems are binary classification scenarios where only few or no minority class samples are available. In order to address both of these cases, we introduce a hyperparameter (c) which sets the CIR of the batch sampled for the inner updates. Hereby, c gives the percentage of the samples belonging to the minority (anomalous) class w.r.t. the total number of samples, e.g. setting $c = 0\%$ means only majority class samples are contained in the data batch. We focus on this latter extreme case, where no anomalous samples are available for learning. In order to evaluate the performance of the adapted model on both classes, we use a *class-balanced* validation batch B' for the meta-updates. This way, we maximize the performance of the model in recognizing both classes after having *seen* examples from only one class during adaptation. The OC-MAML meta-training is described in Algorithm 1 in Appendix A. We note that the proposed episode sampling strategy, i.e. training on a one-class batch then using the loss computed on a class-balanced validation batch to update the meta-learning strategy (e.g. model initialization), is applicable to multiple meta-learning algorithms (Table 3). Using OCC tasks for adaptation during meta-training favors model initializations that enable a quick adaptation to OCC tasks over those that require CB tasks. The schematic visualization in Figure ?? shows the difference between the model initializations meta-learned by MAML and OC-MAML. Hereby, we consider the adaptation to an unseen binary classification task T_s . $\theta_{s,CB}^*$ denotes a local optimum of T_s . The parameter initializations yielded by OC-MAML and MAML are denoted by θ_{OCMAML} and θ_{MAML} respectively. When starting from the OC-MAML parameter initialization, taking a gradient step using an OC support set $D_{s,OC}$ (gradient direction denoted by $\nabla L_{s,OC}$), yields a performance increase on T_s (by moving closer to the local optimum). In contrast, when starting from the parameter initialization reached by MAML, a class-balanced support set $D_{s,CB}$ (gradient direction denoted by $\nabla L_{s,CB}$) is required for a performance increase in T_s .

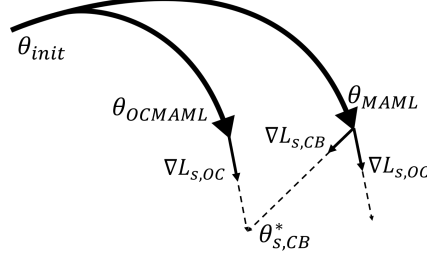


Figure 1: Adaptation to task T_s from the model initializations yielded by OC-MAML and MAML

2.3.2 Theoretical Analysis: Why does OC-MAML work ?

In this section we give a theoretical explanation of why OC-MAML works and why it is a more suitable approach than MAML for the few-shot one-class classification (FS-OCC) problem. To address the latter problem, we aim to find a model parameter initialization, from which adaptation using few data examples from only *one* class yields a good performance on both classes, i.e. good generalization to the class-balanced task. We additionally demonstrate that adapting first-order meta-learning algorithms, e.g. First-Order MAML (FOMAML) [10] and Reptile [32], to the OCC scenario as done in OC-MAML, does not yield initializations with the desired characteristics.

By using a Taylor series expansion the gradient used in the MAML update can be approximated to Equation 2 [32], where the case with only 2 gradient-based updates is considered, i.e. one adaptation update on a minibatch (1) including K datapoints from D^{tr} and one meta-update on a minibatch (2) including Q datapoints from D^{val} . We use the same notation as in [32], where \bar{g}_i and \bar{H}_i denote the gradient and Hessian computed on the i^{th} minibatch at the initial parameter point ϕ_1 , and α gives the learning rate. Here it is assumed that the same learning rate is used for the adaptation and meta-updates.

$$\begin{aligned} g_{MAML} &= \bar{g}_2 - \alpha \bar{H}_2 \bar{g}_1 - \alpha \bar{H}_1 \bar{g}_2 + O(\alpha^2) \\ &= \bar{g}_2 - \alpha \frac{\partial(\bar{g}_1 \cdot \bar{g}_2)}{\partial \phi_1} + O(\alpha^2) \end{aligned} \quad (2)$$

Equation 2 shows that MAML maximizes the inner product of the gradients computed on different minibatches [32]. Under the assumption of local linearity of the loss function (which is the case around small optimization steps), and when gradients from different minibatches have a positive inner product, taking a gradient step using one minibatch yields a performance increase on the other [32]. Maximizing the inner product leads to a decrease in the angle between the gradient vectors and thus to an increase in their cosine similarity. Hence, MAML optimizes for an initialization where gradients computed on *small* minibatches have similar directions, which enables few-shot learning.

Equation 2 is independent of the data strategy adopted and hence holds also for OC-MAML. However, in OC-MAML the minibatches 1 and 2 have different class-imbalance rates (CIRs), since the first minibatch includes examples from only one class and the second minibatch is class-balanced. So, it optimizes for increasing the inner product between a gradient computed on a one-class minibatch and a gradient computed on class-balanced data. Thus, OC-MAML optimizes for an initialization where gradients computed on one-class data have similar directions, i.e. a high inner product and therefore a high cosine similarity, to gradients computed on class-balanced data (Figure ??). Consequently, taking one (or few) gradient step(s) with one-class minibatch(es) from such a parameter initialization results in a performance increase on class-balanced data. This enables one-class classification. In contrast, MAML uses only class-balanced data during meta-training which leads to a parameter initialization that requires class-balanced minibatches to yield the same effect. When adapting to OCC tasks, however, only examples from one class are available. We conclude, therefore, that the proposed data sampling technique modifies MAML to learn parameter initializations that are more suitable for adapting to OCC tasks.

A natural question is whether applying the same data sampling method to other gradient-based meta-learning algorithms would yield the same desired effect. We investigate this for First-Order MAML (FOMAML) [10] and Reptile [32]. FOMAML is a first-order approximation of MAML, which ignores the second derivative terms. Reptile is also a first-order meta-learning algorithm that

learns an initialization that enables fast adaptation to test tasks using only few examples from *each* class. We refer to the versions of these algorithms adapted to the FS-OCC setting as OC-FOMAML and OC-Reptile. We note that for OC-Reptile, the first $(N - 1)$ batches contain examples from only one class and the last (N^{th}) batch is class-balanced. The approximated gradients used in the FOMAML and Reptile updates are given by Equations 3 and 4 [32], respectively.

$$g_{FOMAML} = \bar{g}_2 - \alpha \bar{H}_2 \bar{g}_1 + O(\alpha^2) \quad (3)$$

$$g_{Reptile} = \bar{g}_1 + \bar{g}_2 - \alpha \bar{H}_2 \bar{g}_1 + O(\alpha^2) \quad (4)$$

We note that these equations hold also for OC-FOMAML and OC-Reptile. By taking the expectation over minibatch sampling $\mathbb{E}_{\tau,1,2}$ for a task τ and two *class-balanced* minibatches 1 and 2, it is established that $\mathbb{E}_{\tau,1,2}[\bar{H}_1 \bar{g}_2] = \mathbb{E}_{\tau,1,2}[\bar{H}_2 \bar{g}_1]$ [32]. Averaging the two sides of the latter equation results in

$$\begin{aligned} \mathbb{E}_{\tau,1,2}[\bar{H}_2 \bar{g}_1] &= \frac{1}{2} \mathbb{E}_{\tau,1,2}[\bar{H}_1 \bar{g}_2 + \bar{H}_2 \bar{g}_1] \\ &= \frac{1}{2} \mathbb{E}_{\tau,1,2} \left[\frac{\partial(\bar{g}_1 \cdot \bar{g}_2)}{\partial \phi_1} \right]. \end{aligned} \quad (5)$$

Equation 5 shows that, FOMAML and Reptile, like MAML, in expectation optimize for increasing the inner product of the gradients computed on different minibatches with the *same* CIR. However, when the minibatches 1 and 2 have different CIRs, which is the case for OC-FOMAML and OC-Reptile, $\mathbb{E}_{\tau,1,2}[\bar{H}_1 \bar{g}_2] \neq \mathbb{E}_{\tau,1,2}[\bar{H}_2 \bar{g}_1]$ and therefore $\mathbb{E}_{\tau,1,2}[\bar{H}_2 \bar{g}_1] \neq \frac{1}{2} \mathbb{E}_{\tau,1,2} \left[\frac{\partial(\bar{g}_1 \cdot \bar{g}_2)}{\partial \phi_1} \right]$. Hence, despite using the same data sampling method as OC-MAML, OC-FOMAML and OC-Reptile do *not* explicitly optimize for increasing the inner product, and therefore cosine similarity, between gradients computed on one-class and class-balanced minibatches. The second derivative term $\bar{H}_1 \bar{g}_2$ is, thus, necessary to optimize for an initialization from which performance increase on a class-balanced task is yielded by taking few gradient steps using one class data.

3 Related works

Our proposed method addresses the few-shot one-class classification (FS-OCC) problem, i.e. solving binary classification problems using only *few* datapoints from only *one* class. To the best of our knowledge, this problem was only addressed in [22] and [23], and exclusively in the image data domain. In [22] a feed-forward neural network is trained on ILSVRC 2012 to learn a transformation from feature vectors, extracted by a CNN pre-trained on ILSVRC 2014 [39], to SVM decision boundaries. At test time, an SVM boundary is inferred by using one image of one class from the test task which is then used to classify the test examples. This approach is specific to the image domain since it relies on the availability of very large, well annotated datasets and uses data augmentation techniques specific to the image domain, e.g. mirroring. Meta-learning algorithms offer a more general approach to FS-OCC since they are data-domain-agnostic, and do not require a pre-trained feature extraction model, which not be available for some data domains, e.g. sensor readings. The concurrent work [23] adapts Prototypical Networks [47] to address the FS-OCC problem by using 0 as a prototype for the *null* class, i.e. non-normal examples, since the embedding space is 0-centered due to using batch normalization (BN) [17] as the last layer. Given the embedding of a query example, its distance to the normal-class prototype is then compared to its norm. This method imposes a constraint on the model architecture by requiring the usage of BN layers, which leads to substantial performance decrease when used for some datasets, as shown in our results on the time-series datasets (Table 7). We propose a model-architecture agnostic data sampling technique to adapt meta-learning algorithms to the FS-OCC problem.

3.1 Class-balanced few-shot classification

Meta-learning approaches for FS classification approaches may be broadly categorized in 2 categories. Optimization-based approaches aim to learn an optimization algorithm [37] and/or a parameter

initialization [10, 32], learning rates [29], an embedding network [27] that are tailored for FS learning. Metric-based techniques learn a metric space where samples belonging to the same class are close together, which facilitates few-shot classification [21, 52, 47, 48, 33, 27]. Hybrid methods [40, 28] that combine the advantages of both categories were also developed. Prior meta-learning approaches to FS classification addressed the N -way K -shot classification problem described in Section 2.1, i.e. they require examples from *each* class of the test tasks. We propose a method to adapt meta-learning algorithm to the 1 -way K -shot scenario, where only few examples from *one* class are available.

3.2 One-class classification

Classical OCC approaches rely on SVMs [44, 50] to distinguish between normal and abnormal samples. Hybrid approaches combining SVM-based techniques with feature extractors were developed to compress the input data in lower dimensional representations [53, 9, 4]. Fully deep methods that jointly perform the feature extraction step and the OCC step have also been developed [38]. Another category of approaches to OCC uses the reconstruction error of autoencoders [15] trained with only normal examples as an anomaly score [14, 3, 8]. Yet, determining a decision threshold for such an anomaly score requires labeled data from both classes. Other techniques rely on GANs [13] to perform OCC [42, 36, 41]. The aforementioned hybrid and fully deep approaches require a considerable amount of data from the OCC task to train the typically highly parametrized feature extractors specific to the normal class, and hence fail in the scarce data regime as we empirically show in Appendix D..

4 Experimental evaluation

The conducted experiments ¹ aim to address the following key questions: (a) How do meta-learning-based approaches using the proposed episode sampling technique perform compared to classical one-class classification (OCC) approaches in the few-shot (FS) data regime? (b) Do our theoretical findings (Section 2.3.2) about the differences between the MAML and OC-MAML initializations hold in practice? (c) Does the proposed episode sampling strategy to adapt MAML to the FS-OCC setting yield the expected performance increase and does this hold for further meta-learning algorithms?

4.1 Baselines and Datasets

We compare our adapted version of MAML (OC-MAML) to one-class classification (OCC) with the classical OCC approaches One-Class SVM (OC-SVM) [44] and Isolation Forest (IF) [30] (Question (a)), which we fit to raw features and embeddings of the support set of the test task. Here, we explore two types of embeddings networks which are trained on the meta-training tasks as follows: one is trained in a Multi-Task-Learning (MTL) [6] setting using one-class-vs-all tasks and the other trained using the "Finetune" baseline (FB) [51]. i.e. using multi-class classification on all classes available. Moreover, we compare first-order (FOMAML and Reptile) and second-order (MAML) class-balanced meta-learning algorithms to their adapted versions to the OCC scenario, i.e. OC-FOMAML and OC-Reptile and OC-MAML (Question (b)). Finally, we compare MetaOptNet [27] and meta-SGD [29] to their one-class counterparts that use our sampling strategy (Question c). We conducted a hyperparameter search for each baseline separately and used the best performing setting for our experiments. Experimental details about all the baselines are provided in Appendix B.

We evaluate our approach on 8 datasets from the image and time-series data domains. From the image domain we use 4 few-shot learning benchmarks, namely MiniImageNet [37], Omniglot [25], CIFAR-FS [5] and FC100 [33] and 1 OCC benchmark dataset, the Multi-Task MNIST (MT-MNIST) dataset. To adapt the datasets to the OCC scenario, we create binary classification tasks, where the normal class contains examples from one class of the initial dataset and the anomalous class contains examples from *multiple* other classes. We create 9 sub-datasets based on MNIST, where the meta-testing task of each consists in differentiating between a certain digit and the others, and the same (10^{th}) task for meta-validation in all sub-datasets.

Since most of the time-series datasets for anomaly detection include data from only one domain and only one normal class, it is not possible them to the meta-learning problem formulation where several different tasks are required. Therefore, we create two synthetic time-series (STS) datasets,

¹The code for our experiments will be made public upon paper acceptance.

each including 30 synthetically generated time-series that underlie 30 different anomaly detection tasks. The time-series underlying the datasets are sawtooth waveforms (STS-Sawtooth) and sine functions (STS-Sine). We propose the STS-datasets as benchmark datasets for the few-shot (one-class) classification problem in the time-series domain and will publish them upon paper acceptance. Finally, we validate OC-MAML on a real-world anomaly detection dataset of sensor readings recorded during industrial manufacturing using a CNC milling machine. Various consecutive roughing and finishing operations (pockets, edges, holes, surface finish) were performed on ca. 100 aluminium workpieces to record the CNC Milling Machine Data (CNC-MMD). The temporal dimension is handled using 1-D convolutions. In Appendix C, we give details about all datasets, the task creation procedures adopted to adapt them to the OCC case, as well as the generation of the STS-datasets.

4.2 Results and Discussion

Our results of the comparison between OC-MAML and the classical OCC approaches on 3 image datasets and on the STS-Sawtooth dataset are summarized in Table 5 in Appendix D. While classical OCC methods yields chance performance in almost all settings, OC-MAML achieves very high results, consistently outperforming the former across all datasets and on both support set sizes.

Table 1: Test accuracies (in %) computed on the class-balanced test sets of the test tasks of MiniImageNet (MIN), Omniglot (Omn), MT-MNIST with $T_{test} = T_0$ and STS-Sawtooth (Saw).

Support set size	$K = 2$				$K = 10$			
Model \ Dataset	MIN	Omn	MNIST	Saw	MIN	Omn	MNIST	Saw
Reptile	51.6	56.3	71.1	69.1	57.1	76.3	89.8	81.6
FOMAML	53.3	78.8	80.7	75.1	59.5	93.7	91.1	80.2
MAML	62.3	91.4	85.5	81.1	65.5	96.3	92.2	86
OC-Reptile	51.9	52.1	51.3	51.6	53.2	51	51.4	53.2
OC-FOMAML	55.7	74.7	79.1	58.6	66.1	87.5	91.8	73.2
OC-MAML (ours)	69.1	96.6	88	96.6	76.2	97.6	95.1	95.7

We compare MAML, FOMAML, Reptile and their one-class versions using models with and without BN layers and average over 5 seeds. Table 1 shows the results of the best architecture on 3 image datasets and on the STS-Sawtooth dataset. The results of the 6 meta-learning algorithms using both architectures, as well as the results on the other 8 MT-MNIST task-combinations and on the STS-Sine dataset, are presented in Appendix D and are consistent with the results in Table 1. We observe that OC-MAML consistently outperforms the class-balanced and one-class versions of the meta-learning algorithms, with a substantial margin on all datasets and for both support set sizes, showing the benefits of our modification to MAML.

Moreover, OC-FOMAML and OC-Reptile yield poor results, especially without BN, confirming our findings (Section 2.3.2) that adapting first-order meta-learning algorithms to the OCC setting does not yield the desired effect. We find that using BN yields a substantial performance increase on the 3 image datasets (Table 7) and explain that by the gradient orthogonalizing effect of BN [49]. In fact, gradient orthogonalization reduces interference between gradients computed on one-class and class-balanced batches. OC-MAML achieves competitive results without BN, as it reduces interference between these gradients by the means of its optimization objective (Section 2.3.2).

Validation on the CNC-milling real-world dataset

We validate OC-MAML on the industrial sensor readings dataset CNC-MDD and report the results in Appendix D. We compute F1-scores for evaluation since the test sets are class-imbalanced. Depending on the type of the target milling operation (e.g. roughing), tasks creating from *different* operations from the same type are used for meta-training. OC-MAML consistently achieves high F1-scores between 80% and 95.9% across the 6 milling processes. The high performance on the minority class, i.e. in detecting anomalous data samples, is reached by using only $K = 10$ non-anomalous examples ($c = 0\%$). These results show that OC-MAML yielded a parameter initialization suitable for learning OCC tasks in the time-series data domain and the maturity of this method for industrial real-world applications. Due to the low number of anomalies, it is not possible to apply MAML with the standard sampling, which requires K anomalous examples in the inner loop during meta-training.

Cosine similarity analysis

We would like to directly verify that OC-MAML maximizes the inner product, and therefore the cosine similarity, between the gradients of one-class and class-balanced batches of data, while the other meta-learning baselines do not (Figure ??, Section 2.3.2). For this, we use the initialization meta-learned by each algorithm to compute the loss gradient of K normal examples and the loss gradient of a disjoint class-balanced batch. We use the best performing initialization for each meta-learning algorithm and compute the cosine similarities using on meta-testing tasks.

Table 2: Cosine similarity between the gradients of one-class and class-balanced minibatches averaged over test tasks of MiniImageNet (MIN), Omniglot (Omn), MT-MNIST and STS-Sawtooth (Saw).

Model \ Dataset	MIN	Omn	MNIST	Saw
Reptile	0.05	0.02	0.16	0.02
FOMAML	0.13	0.14	0.31	-0.02
MAML	0.28	0.16	0.45	0.01
OC-Reptile	0.09	0.05	-0.09	0.03
OC-FOMAML	0.26	0.12	0.36	0.07
OC-MAML	0.42	0.23	0.47	0.92

We report the mean cosine similarity on 3 image datasets and one time-series dataset in Table 2. The significant difference in the mean cosine similarity found between OC-MAML and the other meta-learning algorithms consolidate our theoretical findings from section 2.3.2.

Applicability to further metalearning algorithms

To investigate whether the benefits of our sampling strategy generalize to other meta-learning algorithms beyond MAML, we apply it to MetaOptNet [27] and Meta-SGD [29]. MetaOptNet learns feature embeddings that generalize well in the FS regime when fed to linear classifiers, e.g. SVMs. To adapt it to OCC, we fit an OC-SVM [45] on top of the representations extracted for few normal examples by the embedding network, which is then used to classify the class-balanced validation set. Its error is then used to update the embedding network, analogously to the class-balanced scenario. To fit the OC-SVM, we solve its dual problem [45] using the differentiable quadratic programming (QP) solver [2] used to solve the multi-class SVM in [27]. The ResNet12 architecture is used for the embedding network. Meta-SGD learns an update direction and a learning rate for each model parameter besides the initialization. Our episode sampling method is applied as done for MAML.

Table 3: Test accuracies (in %) computed on the class-balanced test sets of the test tasks of MiniImageNet (MIN), CIFAR-FS and FC100 after using a one-class support set for task-specific adaptation

Support set size	$K = 2$			$K = 10$		
Model \ Dataset	MIN	CIFAR-FS	FC100	MIN	CIFAR-FS	FC100
MAML	62.3	62.1	55.1	65.5	69.1	61.6
OC-MAML (ours)	69.1	70	59.9	76.2	79.1	65.5
MetaSGD	65	58.4	55	73.6	71.3	61.3
OC-MetaSGD (ours)	70	70.8	60.3	76.5	79.2	65.3
MetaOptNet	50	56	51.2	56.6	74.8	53.3
OC-MetaOptNet (ours)	51.8	56.3	52.2	67.4	75.5	59.9

Table 3 shows that applying the proposed sampling technique to MetaOptNet and Meta-SGD results in a significant increase in accuracy in the FS-OCC setting on MiniImageNet, CIFAR-FS and FC100 datasets. Eventhough MetaOptNet substantially outperforms MAML and Meta-SGD in the class-balanced case [27], it fails to compete in the FS-OCC setting, suggesting that meta-learning a suitable initialization for the classifier is important in this scenario.

5 Conclusion

This work addressed the novel and challenging problem of few-shot one-class classification (FS-OCC). We proposed an episode generation technique to adapt meta-learning algorithms designed for class-balanced few-shot classification to FS-OCC. Our experiments on eight datasets from the image

and time-series domains, including a real-world dataset of industrial sensor readings, showed that our approach yields substantial performance increase on three meta-learning algorithms, significantly outperforming classical OCC methods and few-shot classification algorithms using standard sampling. Moreover, we provided a theoretical analysis showing that classical gradient-based meta-learning algorithms (e.g. MAML) do not yield model initializations suitable for OCC tasks and that second-order derivatives are needed to optimize for such initializations. Future works could investigate an unsupervised approach to FS-OCC, as done in the class-balanced scenario [16].

Broader Impact

We proposed a very general method for tackling anomaly detection problems in the face of extreme data scarcity and label imbalance.

Anomaly detection has a broad range of application domains but in addition, a large portion of these domains naturally suffer from the data scarcity issue. Large-scale data labeling is not feasible in many of these cases since often a profound amount of domain knowledge is required to analyze and annotate the data for learning. This fact makes a large portion of the current research in AI, which relies on massive amounts of annotated data, not applicable to these domains.

Our motivation for researching our method originates from the industrial domain, in particular the monitoring of workpiece quality during manufacturing.

Naturally, production plants are very efficient and produce only low amounts of anomalies/scrap. Nevertheless, accidentally delivering malicious workpieces can not only harm the reputation of the manufacturer, but also result in massive penalties as well as lead to unexpected behavior of the end product (which might endanger its user). In addition, there is an ever-changing portfolio of workpieces that are manufactured for which no large sets of labeled historical data will be available.

In many production settings, where a manual inspection of the produced workpieces is feasible, quality control often falls into the responsibility of the machine operator and dedicated quality management personnel. In principle, our method could be used to fully automate this task in the long run.

In a broader sense, we proposed a method for tackling anomaly detection problems, which is a very general use case in many domains. As the term “anomaly” is very ambiguous and subjective our method can be misused for detecting any kind of such, given the data for learning these “anomalies” has a sufficiently high quality. Naturally, our method is biased towards the data that is provided for learning and cannot automatically counteract any ethical violations. As an example, anomaly detectors can be the basis of applications that discriminate individuals based on their available data (images, profiles, etc.).

References

- [1] Charu C Aggarwal. Outlier analysis. In *Data mining*, pages 237–263. Springer, 2015.
- [2] Brandon Amos and J Zico Kolter. Optnet: Differentiable optimization as a layer in neural networks. In *Proceedings of the 34th International Conference on Machine Learning-Volume 70*, pages 136–145. JMLR. org, 2017.
- [3] Jinwon An and Sungzoon Cho. Variational autoencoder based anomaly detection using reconstruction probability. *Special Lecture on IE*, 2:1–18, 2015.
- [4] Jerone TA Andrews, Thomas Tanay, Edward J Morton, and Lewis D Griffin. Transfer representation-learning for anomaly detection. ICML, 2016.
- [5] Luca Bertinetto, Joao F Henriques, Philip HS Torr, and Andrea Vedaldi. Meta-learning with differentiable closed-form solvers. *arXiv preprint arXiv:1805.08136*, 2018.
- [6] Rich Caruana. Multitask learning. *Machine learning*, 28(1):41–75, 1997.
- [7] Varun Chandola, Arindam Banerjee, and Vipin Kumar. Anomaly detection: A survey. *ACM computing surveys (CSUR)*, 41(3):15, 2009.

- [8] Jinghui Chen, Saket Sathe, Charu Aggarwal, and Deepak Turaga. Outlier detection with autoencoder ensembles. In *Proceedings of the 2017 SIAM International Conference on Data Mining*, pages 90–98. SIAM, 2017.
- [9] Sarah M Erfani, Sutharshan Rajasegarar, Shanika Karunasekera, and Christopher Leckie. High-dimensional and large-scale anomaly detection using a linear one-class svm with deep learning. *Pattern Recognition*, 58:121–134, 2016.
- [10] Chelsea Finn, Pieter Abbeel, and Sergey Levine. Model-agnostic meta-learning for fast adaptation of deep networks. In *Proceedings of the 34th International Conference on Machine Learning-Volume 70*, pages 1126–1135. JMLR. org, 2017.
- [11] Chelsea Finn and Sergey Levine. Meta-learning and universality: Deep representations and gradient descent can approximate any learning algorithm, 2017.
- [12] Pedro Garcia-Teodoro, Jesus Diaz-Verdejo, Gabriel Maciá-Fernández, and Enrique Vázquez. Anomaly-based network intrusion detection: Techniques, systems and challenges. *computers & security*, 28(1-2):18–28, 2009.
- [13] Ian Goodfellow, Jean Pouget-Abadie, Mehdi Mirza, Bing Xu, David Warde-Farley, Sherjil Ozair, Aaron Courville, and Yoshua Bengio. Generative adversarial nets. In *Advances in neural information processing systems*, pages 2672–2680, 2014.
- [14] Simon Hawkins, Hongxing He, Graham Williams, and Rohan Baxter. Outlier detection using replicator neural networks. In *International Conference on Data Warehousing and Knowledge Discovery*, pages 170–180. Springer, 2002.
- [15] Geoffrey E Hinton and Ruslan R Salakhutdinov. Reducing the dimensionality of data with neural networks. *science*, 313(5786):504–507, 2006.
- [16] Kyle Hsu, Sergey Levine, and Chelsea Finn. Unsupervised learning via meta-learning, 2018.
- [17] Sergey Ioffe and Christian Szegedy. Batch normalization: Accelerating deep network training by reducing internal covariate shift. *arXiv preprint arXiv:1502.03167*, 2015.
- [18] Eric Jones, Travis Oliphant, Pearu Peterson, et al. SciPy: Open source scientific tools for Python, 2001–. [Online; accessed <today>].
- [19] Shehroz S Khan and Michael G Madden. One-class classification: taxonomy of study and review of techniques. *The Knowledge Engineering Review*, 29(3):345–374, 2014.
- [20] Diederik P Kingma and Jimmy Ba. Adam: A method for stochastic optimization. *arXiv preprint arXiv:1412.6980*, 2014.
- [21] Gregory R. Koch. Siamese neural networks for one-shot image recognition. 2015.
- [22] Jędrzej Koźerawski and Matthew Turk. Clear: Cumulative learning for one-shot one-class image recognition. In *Proceedings of the IEEE Conference on Computer Vision and Pattern Recognition*, pages 3446–3455, 2018.
- [23] Anna Kruspe. One-way prototypical networks. *arXiv preprint arXiv:1906.00820*, 2019.
- [24] Brenden Lake, Ruslan Salakhutdinov, Jason Gross, and Joshua Tenenbaum. One shot learning of simple visual concepts. In *Proceedings of the annual meeting of the cognitive science society*, volume 33, 2011.
- [25] Brenden M. Lake, Ruslan Salakhutdinov, and Joshua B. Tenenbaum. Human-level concept learning through probabilistic program induction. *Science*, 350(6266):1332–1338, 2015.
- [26] Yann LeCun, Corinna Cortes, and Christopher J.C. Burges. The mnist database of handwritten digits, 2010. <http://yann.lecun.com/exdb/mnist/>.
- [27] Kwonjoon Lee, Subhansu Maji, Avinash Ravichandran, and Stefano Soatto. Meta-learning with differentiable convex optimization. In *Proceedings of the IEEE Conference on Computer Vision and Pattern Recognition*, pages 10657–10665, 2019.

- [28] Yoonho Lee and Seungjin Choi. Gradient-based meta-learning with learned layerwise metric and subspace. *arXiv preprint arXiv:1801.05558*, 2018.
- [29] Zhenguo Li, Fengwei Zhou, Fei Chen, and Hang Li. Meta-sgd: Learning to learn quickly for few-shot learning. *arXiv preprint arXiv:1707.09835*, 2017.
- [30] Fei Tony Liu, Kai Ming Ting, and Zhi-Hua Zhou. Isolation forest. In *2008 Eighth IEEE International Conference on Data Mining*, pages 413–422. IEEE, 2008.
- [31] Mary M Moya, Mark W Koch, and Larry D Hostetler. One-class classifier networks for target recognition applications. *NASA STI/Recon Technical Report N*, 93, 1993.
- [32] Alex Nichol and John Schulman. Reptile: a scalable metalearning algorithm. *arXiv preprint arXiv:1803.02999*, 2018.
- [33] Boris Oreshkin, Pau Rodríguez López, and Alexandre Lacoste. Tadam: Task dependent adaptive metric for improved few-shot learning. In *Advances in Neural Information Processing Systems*, pages 721–731, 2018.
- [34] Marcel Prastawa, Elizabeth Bullitt, Sean Ho, and Guido Gerig. A brain tumor segmentation framework based on outlier detection. *Medical image analysis*, 8(3):275–283, 2004.
- [35] Aniruddh Raghu, Maithra Raghu, Samy Bengio, and Oriol Vinyals. Rapid learning or feature reuse? towards understanding the effectiveness of maml. *arXiv preprint arXiv:1909.09157*, 2019.
- [36] Mahdyar Ravanbakhsh, Moin Nabi, Enver Sangineto, Lucio Marcenaro, Carlo Regazzoni, and Nicu Sebe. Abnormal event detection in videos using generative adversarial nets. *2017 IEEE International Conference on Image Processing (ICIP)*, Sep 2017.
- [37] Sachin Ravi and Hugo Larochelle. Optimization as a model for few-shot learning. 2016.
- [38] Lukas Ruff, Robert Vandermeulen, Nico Goernitz, Lucas Deecke, Shoaib Ahmed Siddiqui, Alexander Binder, Emmanuel Müller, and Marius Kloft. Deep one-class classification. In *International Conference on Machine Learning*, pages 4393–4402, 2018.
- [39] Olga Russakovsky, Jia Deng, Hao Su, Jonathan Krause, Sanjeev Satheesh, Sean Ma, Zhiheng Huang, Andrej Karpathy, Aditya Khosla, Michael Bernstein, Alexander C. Berg, and Li Fei-Fei. ImageNet Large Scale Visual Recognition Challenge. *International Journal of Computer Vision (IJCV)*, 115(3):211–252, 2015.
- [40] Andrei A. Rusu, Dushyant Rao, Jakub Sygnowski, Oriol Vinyals, Razvan Pascanu, Simon Osindero, and Raia Hadsell. Meta-learning with latent embedding optimization, 2018.
- [41] Mohammad Sabokrou, Mohammad Khalooei, Mahmood Fathy, and Ehsan Adeli. Adversarially learned one-class classifier for novelty detection. *2018 IEEE/CVF Conference on Computer Vision and Pattern Recognition*, Jun 2018.
- [42] Thomas Schlegl, Philipp Seeböck, Sebastian M Waldstein, Ursula Schmidt-Erfurth, and Georg Langs. Unsupervised anomaly detection with generative adversarial networks to guide marker discovery. In *International Conference on Information Processing in Medical Imaging*, pages 146–157. Springer, 2017.
- [43] Jürgen Schmidhuber. *Evolutionary principles in self-referential learning, or on learning how to learn: the meta-meta-... hook*. PhD thesis, Technische Universität München, 1987.
- [44] Bernhard Schölkopf, John C Platt, John Shawe-Taylor, Alex J Smola, and Robert C Williamson. Estimating the support of a high-dimensional distribution. *Neural computation*, 13(7):1443–1471, 2001.
- [45] Bernhard Schölkopf, Robert C Williamson, Alex J Smola, John Shawe-Taylor, and John C Platt. Support vector method for novelty detection. In *Advances in neural information processing systems*, pages 582–588, 2000.

- [46] Luke Scime and Jack Beuth. Anomaly detection and classification in a laser powder bed additive manufacturing process using a trained computer vision algorithm. *Additive Manufacturing*, 19:114–126, 2018.
- [47] Jake Snell, Kevin Swersky, and Richard Zemel. Prototypical networks for few-shot learning. In *Advances in Neural Information Processing Systems*, pages 4077–4087, 2017.
- [48] Flood Sung, Yongxin Yang, Li Zhang, Tao Xiang, Philip H.S. Torr, and Timothy M. Hospedales. Learning to compare: Relation network for few-shot learning. In *The IEEE Conference on Computer Vision and Pattern Recognition (CVPR)*, June 2018.
- [49] Mihai Suteu and Yike Guo. Regularizing deep multi-task networks using orthogonal gradients. *arXiv preprint arXiv:1912.06844*, 2019.
- [50] David MJ Tax and Robert PW Duin. Support vector data description. *Machine learning*, 54(1):45–66, 2004.
- [51] Eleni Triantafillou, Tyler Zhu, Vincent Dumoulin, Pascal Lamblin, Kelvin Xu, Ross Goroshin, Carles Gelada, Kevin Swersky, Pierre-Antoine Manzagol, and Hugo Larochelle. Meta-dataset: A dataset of datasets for learning to learn from few examples. *CoRR*, abs/1903.03096, 2019.
- [52] Oriol Vinyals, Charles Blundell, Timothy Lillicrap, Koray Kavukcuoglu, and Daan Wierstra. Matching networks for one shot learning, 2016.
- [53] Dan Xu, Elisa Ricci, Yan Yan, Jingkuan Song, and Nicu Sebe. Learning deep representations of appearance and motion for anomalous event detection. *Proceedings of the British Machine Vision Conference 2015*, 2015.

A OC-MAML: Algorithm and Parameter Initialization

In this section we present the pseudo-code of OC-MAML in Algorithm 1.

Algorithm 1 Meta-training of OC-MAML

Require: S^{tr} : Set of meta-training tasks
Require: α, β : Learning rates
Require: K, Q : Batch size for the inner and outer updates
Require: c : CIR for the inner-updates

- 1: Randomly initialize θ
- 2: **while** not done **do**
- 3: Sample batch of tasks T_i from S^{tr}
 Let $\{D^{tr}, D^{val}\} = T_i$
- 4: **for all** sampled T_i **do**
- 5: Sample K datapoints $B = \{\mathbf{x}^{(l)}, \mathbf{y}^{(l)}\}$ from D^{tr} such that CIR= c
- 6: Initialize $\theta'_i = \theta$
- 7: **for** number of adaptation steps **do**
- 8: Compute adaptation loss $L_{T_i}^{tr}(f_{\theta'_i})$ using B
- 9: Compute adapted parameters with gradient descent: $\theta'_i = \theta'_i - \alpha \nabla_{\theta'_i} L_{T_i}^{tr}(f_{\theta'_i})$
- 10: **end for**
- 11: Sample Q datapoints $B' = \{\mathbf{x}'^{(l)}, \mathbf{y}'^{(l)}\}$ from D^{val} such that CIR= 50%
- 12: Compute outer loop loss $L_{T_i}^{val}(f_{\theta'_i})$ using B'
- 13: **end for**
- 14: Update θ : $\theta \leftarrow \theta - \beta \nabla_{\theta} \sum_{T_i} L_{T_i}^{val}(f_{\theta'_i})$
- 15: **end while**
- 16: **return** meta-learned parameters θ

B Experiment Details

For MT-MNIST, we use the same 4-block convolutional architecture as used by [16] for their multi-class MNIST experiments. Each convolutional block includes a 3 x 3 convolutional layer with 32 filters, a 2 x 2 pooling and a ReLU non-linearity. The same model architecture is used for the MiniImageNet experiments as done by [37]. For the Omniglot experiments, we use the same architecture used by [10]. We also do not include the batch normalization layers for the two latter datasets.

On the STS datasets, the model architecture used is composed of 3 modules, each including a 5 x 5 convolutional layer with 32 filters, a 2 x 2 pooling and a ReLU non-linearity. The model architecture used for the CNC-MMD experiments is composed of 4 of these aforementioned modules, except that the convolutional layers in the last two modules include 64 filters. The last layer of all architectures is a linear layer followed by softmax. We note that in the experiments on the time-series datasets (STS and CNC-MMD) 1-D convolutional filters are used.

We conducted a hyperparameter grid search for each meta-learning algorithm separately. The hyperparameters with the most effect on the algorithm performance were identified and varied. These are: the inner and outer learning rates (α and β), the number of inner updates (adaptation steps). We also conducted a separate hyperparameter search for the case, where BN layers are used. Our results are averaged over 5 runs with different seeds, using the best hyperparameter values. For the outer learning rate β we searched over the grid $\{0.1, 0.01, 0.001\}$ for all datasets. Regarding the inner learning rate (α) we searched over the grids $\{0.1, 0.01, 0.001\}$ for MiniImageNet and the STS datasets, and $\{0.1, 0.05, 0.01\}$ for MT-MNIST and Omniglot. As for the number of adaptation steps, we search over the grids $\{1, 3, 5\}$ for MiniImageNet, MT-MNIST and Omniglot, and $\{1, 3, 5, 10\}$ for the STS datasets.

For the meta-learning algorithms, including OC-MAML, we used vanilla SGD in the inner loop and the Adam optimizer [20] in the outer loop, as done by [10]. For (FO)MAML and OC-(FO)MAML,

the size of the query set, also called outer loop minibatch, (Q), was set to 60, 20, 100 and 50, for MiniImageNet, Omniglot, MT-MNIST and the STS datasets respectively. Since the outer loop data is class-balanced, it includes $Q/2$ examples per class. Reptile uses the same batch size for all updates [32]. Hence, we set the outer loop minibatch size to be equal to the inner loop minibatch size, i.e. $Q = K$. The number of meta-training tasks used in each meta-training iteration (also called meta-batch size) was set to 8 for all datasets.

The MTL and FB baselines were also trained with the Adam optimizer. Here, the batch size used is 32 for all datasets, and the learning rate was set to 0.05 for MiniImageNet and Omniglot and 0.01 for MT-MNIST and STS.

In the following we give the hyperparameters used for the real-world CNC-MMD dataset of industrial sensor readings. The outer learning rate (β) was set to 0.001, the inner learning rate (α) was set to 0.0001, the number of adaptation steps was set to 5 and the meta-batch size was set to 16. Since the sizes and CIRS of the validation sets D^{val} differ across the meta-training tasks in this dataset, we could not fix the outer loop size Q . Here we sample the Q datapoints with the biggest possible size, under the constraint that these datapoints are class-balanced. The resulting Q values are between 4 and 16, depending on the meta-training task.

In the following, we provide details about the meta-training procedure adopted in the meta-learning experiments. We use disjoint sets of data for adaptation (D^{tr}) and validation (D^{val}) on the meta-training tasks, as it was empirically found to yield better final performance [32]. Hereby, the same sets of data are used in the OC-MAML and baseline experiments. In the MT-MNIST, Omniglot, MiniImageNet and STS experiments, the aforementioned sets of data are class-balanced. The sampling of the batch used for adaptation B ensures that this latter has the appropriate CIR ($c = 50\%$ for MAML, FOMAML and Reptile, and $c = c_{target}$ for OC-MAML, OC-FOMAML and OC-Reptile). For the one-class meta-learning algorithms, $c_{target} = 0\%$, i.e. no anomalous samples of the target task are available, so that only normal examples are sampled from D^{tr} during meta-training. In order to ensure that class-balanced and one-class meta-learning algorithms are exposed to the same data during meta-training, we move the anomalous examples from the adaptation set of data (D^{tr}) to the validation set of data (D^{val}). We note that this is only done in the experiments using one-class meta-learning algorithms.

During meta-training, meta-validation episodes are conducted to perform model selection. In order to mimic the adaptation to unseen FS-OCC tasks with CIR $c = c_{target}$ at test time, the CIR of the batches used for adaptation during meta-validation episodes is also set to $c = c_{target}$. We note that the hyperparameter K denotes the total number of datapoints, i.e. batch size, used to perform the adaptation updates, and not the number of datapoints *per class* as done by [10]. Hence, a task with size $K = 10$ and CIR $c = 50\%$ is equivalent to a 2-way 5-shot classification task.

In the following, we provide details about the adaptation to the target task(s) and the subsequent evaluation. In the MT-MNIST and MiniImageNet experiments, we randomly sample 20 adaptation sets from the target task(s)' data, each including K examples with the CIR corresponding to the experiment considered. After each adaptation episode conducted using one of these sets, the adapted model is evaluated on a disjoint class-balanced test set that includes 4,000 images for MT-MNIST and 600 for MiniImageNet. We note that the samples included in the test sets of the test tasks are not used nor for meta-training neither for meta-validation. This results in 20 and 400 (20 adaptation sets created from each of the 20 test classes) different test tasks for MT-MNIST and MiniImageNet, respectively. All the results presented give the mean over all adaptation episodes. Likewise, in the STS experiments, we evaluate the model on 10 different adaptation sets from each of the 5 test tasks. In the CNC-MMD experiments, the 30 tasks created from the target operation are used for adaptation and subsequent evaluation. For each of these target tasks, we randomly sample K datapoints belonging to the normal class that we use for adaptation, and use the rest of the datapoints for testing. We do this 5 times for each target task, which results in 150 testing tasks. For MTL and FB baselines, as well as all the baseline combining these model with shallow models, i.e. IF and OC-SVM, we use the meta-validation task(s) for model choice, like in the meta-learning experiments. For the MTL baseline, for each validation task, we finetune a fully connected layer on top of the shared multi-task learned layers, as it is done at test time.

C Datasets and task creation procedures

In this Section we provide information about the datasets used and the task creation procedures.

Multi-task MNIST (MT-MNIST): We derive 10 binary classification tasks from the MNIST dataset [26], where every task consists in recognizing one of the digits. This is a classical one-class classification benchmark dataset. For a particular task T_i , images of the digit i are labeled as normal samples, while out-of-distribution samples, i.e. the other digits, are labeled as anomalous samples. We use 8 tasks for meta-training, 1 for meta-validation and 1 for meta-testing. Hereby, images of digits to be recognized in the validation and test tasks are not used as anomalies in the meta-training tasks. This ensures that the model is not exposed to normal samples from the test task during meta-training. Moreover, the sets of anomalous samples of the meta-training, meta-validation and meta-testing tasks are mutually disjoint. We conduct experiments on 9 MT-MNIST datasets, each of which involves a different target task ($T_0 - T_8$). The task T_9 is used as a meta-validation task across all experiments. Each image has the shape 28x28.

Omniplot: This dataset was proposed in [25] and includes 20 instances of 1623 hand-written characters from 50 different alphabets. We generate our meta-training and meta-testing tasks based on the official data split [25], where 30 alphabets are reserved for training and 20 for evaluation. For each character class, we create a binary classification task, which consists in differentiating between this character and other characters from the same set (meta-training or meta-testing), i.e. the anomalous examples of a task T_i are randomly sampled from the remaining characters. By removing 80 randomly sampled tasks from the meta-training tasks, we create the meta-validation tasks set. Each image has the shape 28x28.

MiniImageNet: This dataset was proposed in [37] and includes 64 classes for training, 16 for validation and 20 for testing, and is a classical challenging benchmark dataset for few-shot learning. 600 images per class are available. To adapt it to the few-shot *one-class* classification setting, we create 64 binary classification tasks for meta-training, each of which consists in differentiating one of the training classes from the others, i.e. the anomalous examples of a task T_i are randomly sampled from the 63 classes with labels different from i . We do the same to create 16 meta-validation and 20 meta-testing tasks using the corresponding classes. Each image has the shape 84x84x3.

CIFAR-FS: This dataset was proposed in [5] and includes 64 classes for training, 16 for validation and 20 for testing, derived from CIFAR-100, and is a benchmark dataset for few-shot learning. 600 images of size 32x32x3 are available per class. To adapt it to the few-shot *one-class* classification setting, we proceeded exactly as we did for miniImageNet (see above).

FC100: This dataset was proposed in [33] and also includes 64 classes for training, 16 for validation and 20 for testing derived from CIFAR-100, and is a benchmark dataset for few-shot learning. However, in this dataset, the classes for training, validation and testing belong to different superclasses to minimize semantic overlap. This dataset contains 600 images of size 32x32x3 per class. To adapt it to the few-shot *one-class* classification setting, we proceeded exactly as we did for miniImageNet (see above).

Synthetic time-series (STS): In order to investigate the applicability of OC-MAML to time-series (question (c)), we created two datasets, each including 30 synthetically generated time-series that underlie 30 different anomaly detection tasks. The time-series underlying the datasets are sawtooth waveforms (STS-Sawtooth) and sine functions (STS-Sine). Each time-series is generated with random frequencies, amplitudes, noise boundaries, as well as anomaly width and height boundaries. Additionally, the width of the rising ramp as a proportion of the total cycle is sampled randomly for the sawtooth dataset, which results in tasks having rising and falling ramps with different steepness values. The data samples of a particular task are generated by randomly cropping windows of length 128 from the corresponding time-series. We generate 200 normal and 200 anomalous data examples for each task. For each dataset, we randomly choose 20 tasks for meta-training, 5 for meta-validation and 5 for meta-testing. We propose the STS-datasets as benchmark datasets for the few-shot one-class classification problem in the time-series domain, and will make them public upon paper acceptance.

In the following, we give details about the generation procedure adopted to create the STS-Sawtooth dataset. The same steps were conducted to generate the STS-Sine dataset. First, we generate the sawtooth waveforms underlying the different tasks by using the Signal package of the Scipy library [18]. Thereafter, a randomly generated noise is applied to each signal. Subsequently, signal segments

with window length $l = 128$ are randomly sampled from each noisy signal. These represent the normal, i.e. non-anomalous, examples of the corresponding task. Then, some of the normal examples are randomly chosen, and anomalies are added to them to produce the anomalous examples.

Figure 2: Exemplary normal (left) and anomalous (right) samples belonging to different tasks from the STS-Sawtooth (a and b) and the STS-Sine (c and d) datasets

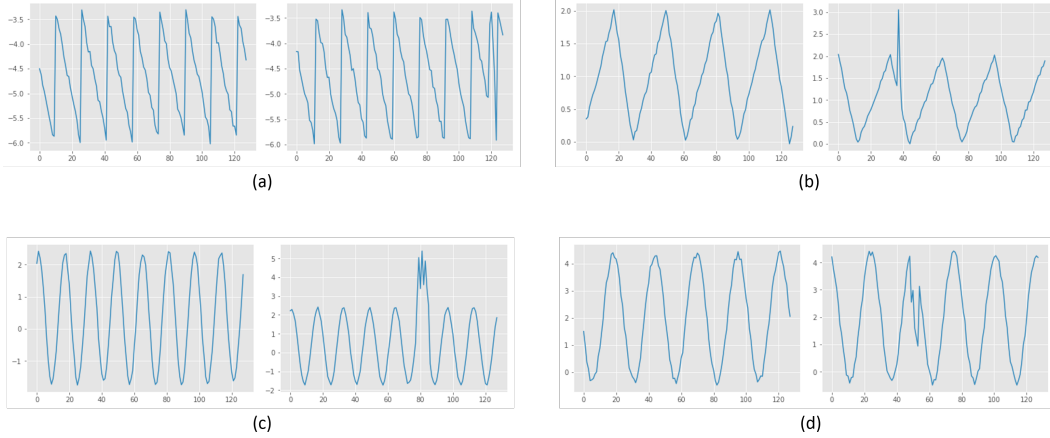


Figure 2 shows exemplary normal and anomalous samples from the STS-Sawtooth and STS-Sine datasets. In order to increase the variance between the aforementioned synthetic signals underlying the different tasks, we randomly sample the frequency, i.e. the number of periods within the window length l , with which each waveform is generated, as well as the amplitude and the vertical position (see Figure 2). For sawtooth waveforms, we also randomly sample the width of the rising ramp as a proportion of the total cycle between 0% and 100%, for each task. Setting this value to 100% and to 0% produces sawtooth waveforms with rising and falling ramps, respectively. Setting it to 50% corresponds to triangle waveforms.

We note that the noise applied to the tasks are randomly sampled from *task-specific* intervals, the boundaries of which are also randomly sampled. Likewise, the width and height of each anomaly is sampled from a random task specific-interval. Moreover, we generate the anomalies of each task, such that half of them have a height between the signal’s minimum and maximum (e.g. anomalies (a) and (d) in Figure 2), while the other half can surpass these boundaries, i.e. the anomaly is higher than the normal signal’s maximum or lower than its minimum at least at one time step (e.g. anomalies (b) and (c) in Figure 2). We note that an anomalous sample can have more than one anomaly.

We preprocess the data by removing the mean and scaling to unit variance. Hereby, only the available *normal* examples are used for the computation of the mean and the variance. This means that in the experiments, where the target task’s size $K = 2$ and only normal samples are available $c = 0\%$, only two examples are used for the mean and variance computation. We note that the time-series in Figure 2 are not preprocessed.

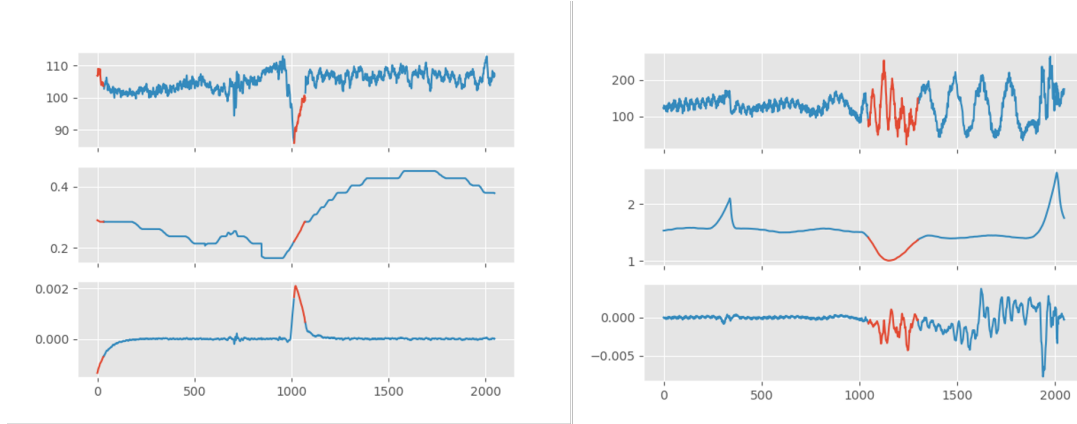
CNC Milling Machine Data (CNC-MMD): This dataset consists of ca. 100 aluminum workpieces on which various consecutive roughing and finishing operations (pockets, edges, holes, surface finish) are performed. The sensor readings which were recorded at a rate of 500Hz measure various quantities that are important for the process monitoring including the torques of the various axes. Each run of machining a single workpiece can be seen as a multivariate time-series. We segmented the data of each run in the various operations performed on the workpieces. E.g. one segment would describe the milling of a pocket where another describes a surface finish operation on the workpiece. Since most manufacturing processes are highly efficient, anomalies are quite rare but can be very costly if undetected. For this reason, anomalies were provoked for 6 operations during manufacturing to provide a better basis for the analysis. Anomalies were provoked by creating realistic scenarios for deficient manufacturing. Examples are using a workpiece that exhibits deficiencies which leads to a drop in the torque signal or using rather slightly decalibrated process parameters which induced various irritations to the workpiece surface which harmed production quality. The data was labeled by domain experts from Siemens Digital Industries. It should be noted that this dataset more realistically

reflects the data situation in many real application scenarios from industry where anomalies are rare and data is scarce and for this reason training models on huge class-balanced datasets is not an option.

For our experiments, we created 30 tasks per operation by randomly cropping windows of length 2048 from the corresponding time-series of each operation. As a result, the data samples of a particular task T_i cropped from a milling operation O_j correspond to the same trajectory part of O_j , but to different workpieces. The task creation procedure ensures that at least two anomalous data samples are available for each task. The resulting tasks include between 15 and 55 normal samples, and between 2 and 4 (9 and 22) anomalous samples for finishing (roughing) operations. We validate our approach on all 6 milling operations in the case where only 10 samples belonging to the normal class ($K = 10$, $c = 0\%$) are available. Given the type of the target milling operation, e.g. finishing, we use the tasks from the other operations of the same type for meta-training. We note that the model is not exposed to any sample belonging to any task of the target operation during training. Each example has the shape 2048x3.

We preprocess each of the three signals separately by removing the mean and scaling to unit variance, as done for the STS datasets. Likewise, only the available *normal* examples are used for the computation of the mean and the variance.

Figure 3: Exemplary anomalous samples from a finishing (left) and a roughing (right) operations, where the anomalous time-steps are depicted in red.



Exemplary anomalous signals recorded from a finishing and a roughing operations are shown in Figure 3. These signals are not mean centered and scaled to unit variance. We note that we do not use the labels per time-step, but rather the label "anomalous" is assigned to each time-series that contains at least an anomalous time-step.

D Experimental Results

In this Section, we present the F1-scores on the CNC-MMD dataset including confidence intervals. Subsequently, we report the results of the experiments on the STS-Sine dataset and the 8 further MT-MNIST task combinations.

On the STS-Sine dataset and the 8 other MT-MNIST task combinations, we observe consistent results with the results from section 4.2. OC-MAML yields high performance across all datasets. For some MT-MNIST task combinations, OC-MAML does not yield the best performance (Tables 8, 10 and 11). This happens only for the MT-MNIST dataset and we explain it by the very high (digit) class overlap between meta-training tasks and the meta-testing task. We also note that none of the meta-learning baselines consistently yields high performance across all datasets, as it is the case for OC-MAML.

Table 4: Test F1-scores of OC-MAML on finishing (F_i) and roughing (R_j) operations of the CNC-MMD dataset, when only $K = 10$ normal examples are available ($c = 0\%$). The \pm shows 95% confidence intervals over 150 tasks sampled from the test operations (not used for meta-training).

F_1	F_2	F_3	F_4	R_1	R_2
$80.0 \pm 2.3\%$	$89.6 \pm 2.1\%$	$95.9 \pm 1.1\%$	$93.6 \pm 3.4\%$	$85.3 \pm 1.4\%$	$82.6 \pm 1.4\%$

Table 5: Test accuracies (in %) computed on the class-balanced test sets of the test tasks of MiniImageNet (MIN), Omniglot (Omni), MT-MNIST with $T_{test} = T_0$ and STS-Sawtooth (Saw). One-class adaptation sets ($c = 0\%$) are used, unless otherwise specified.

Adaptation set size	$K = 2$				$K = 10$			
Model \ Dataset	MIN	Omni	MNIST	Saw	MIN	Omni	MNIST	Saw
FB ($c = 50\%$)	56.2	63.1	65.7	49.8	65.5	73.3	85.7	59.6
MTL ($c = 50\%$)	55.9	50.0	64.6	50.1	63.1	50.0	86.6	50.9
FB	50.0	50.6	56.5	50.0	50.0	51.2	50.3	50.0
MTL	50.0	50.0	49.7	50.0	50.2	50.0	45.3	50.0
OC-SVM	50.2	50.6	51.2	50.1	51.2	50.4	53.6	50.5
IF	50.0	50.0	50.0	50.0	50.7	50.0	50.9	49.9
FB + OCSVM	50.0	50.0	55.5	50.4	51.4	58.0	86.6	58.3
FB + IF	50.0	50.0	50.0	50.0	50.0	50.0	76.1	51.5
MTL + OCSVM	50.0	50.0	50.0	50.0	50.0	50.1	53.8	86.9
MTL + IF	50.0	50.0	50.0	50.0	50.0	55.7	84.2	64.0
OC-MAML (ours)	66.1	90.8	77.8	96.6	71.8	93.7	90.4	95.2

E Speeding up OC-MAML

A concurrent work [35] established that MAML’s rapid learning of new tasks is dominated by feature reuse. The authors propose the Almost No Inner Loop (ANIL) algorithm, which consists in limiting the task-specific adaptation of MAML (inner loop updates) to the parameters of the model’s last layer (the output layer), during meta-training and meta-testing. This leads to a speed up factor of 1.7 over MAML, since ANIL requires the computation of second-order derivative terms only for the last layer’s parameters instead of all parameters. ANIL achieves very comparable performance to MAML.

We investigate, whether this simplification of MAML can also speed up OC-MAML, while retaining the same performance. In other words, could we also compute the second-order derivatives, which are required to explicitly optimize for few-shot one-class classification (FS-OCC) (section 2.3.2), to the last layer’s parameters and still reach a model initialization suitable for FS-OCC. Preliminary results of OC-ANIL on the MiniImageNet and Omniglot datasets were very comparable to the results of OC-MAML. Moreover, we conducted the same cosine similarity analysis described in section 4.2 with ANIL, FOANIL, OC-ANIL and OC-FOANIL and got very consistent results with our findings for the MAML-based algorithms (Table 2). This confirms that second-order derivatives have only to be computed for the last layer of the neural network to optimize for FS-OCC, and that OC-ANIL is faster than OC-MAML by a factor of 1.7 [35] with comparable performance. This modification significantly reduces the computational burden incurred by computing the second-order derivatives for all parameters as done in OC-MAML. Our implementation of OC-ANIL will be published upon paper acceptance.

Table 6: Test accuracies (in %) computed on the class-balanced test sets of the test tasks of the STS-Sine dataset. One-class adaptation sets ($c = 0\%$) are used, unless otherwise specified.

Model \ Adaptation set size	$K = 2$	$K = 10$
FB ($c = 50\%$)	68.9	77.7
MTL ($c = 50\%$)	64.5	91.2
FB	73.8	76.6
MTL	50	50
OC-SVM	50.2	51.3
IF	50	49.9
FB + OCSVM	52.1	65.3
FB + IF	50	62.8
MTL + OCSVM	50	51.9
MTL + IF	50	64.7
OC-MAML (ours)	99.9	99.9

Table 7: Test accuracies (in %) computed on the class-balanced test sets of the test tasks of MiniImageNet (MIN), Omniglot (Omn), MT-MNIST with $T_{test} = T_0$ and STS-Sawtooth (Saw). The results are shown for models without BN (top) and with BN (bottom), and give the average over 5 different seeds. One-class support sets ($c = 0\%$) are used, unless otherwise specified.

Support set size	$K = 2$				$K = 10$			
Model \ Dataset	MIN	Omn	MNIST	Saw	MIN	Omn	MNIST	Saw
Reptile	50.2	50	71.1	50.6	50.2	56.2	85.2	72.8
FOMAML	50	50.9	80.7	52.5	50	50.6	83.8	50.4
MAML	51.4	87.2	80.7	81.1	50	92.3	91.9	72.9
OC-Reptile	50	50.4	50	50	50	50.7	50	50
OC-FOMAML	54.6	52.2	57.5	55.9	51	53.2	73.3	58.9
OC-MAML (ours)	66.4	95.6	85.2	96.6	73	96.8	95.1	95.7
Reptile (BN)	51.6	56.3	61.8	69.1	57.1	76.3	89.8	81.6
FOMAML (BN)	53.3	78.8	80	75.1	59.5	93.7	91.1	80.2
MAML (BN)	62.3	91.4	85.5	51.7	65.5	96.3	92.2	86
OC-Reptile (BN)	51.9	52.1	51.3	51.6	53.2	51	51.4	53.2
OC-FOMAML (BN)	55.7	74.7	79.1	58.6	66.1	87.5	91.8	73.2
OC-MAML (BN) (ours)	69.1	96.6	88	51.3	76.2	97.6	95.1	88.8

Table 8: Test accuracies (in %) computed on the class-balanced test sets of the test tasks of the MT-MNIST datasets with $T_{test} = T_{1-4}$. One-class adaptation sets ($c = 0\%$) are used, unless otherwise specified.

Adaptation set size	$K = 2$				$K = 10$			
Model \ Dataset	1	2	3	4	1	2	3	4
FB ($c = 50\%$)	78.8	59.8	66.7	66.8	91.9	77.3	79.9	81.5
MTL ($c = 50\%$)	64.9	65	59.5	56.4	91	84.6	84.4	83.3
FB	53.7	56	50.7	57.1	53.6	50.7	50.2	59
MTL	54	46.8	41.5	52	49.4	49.6	54.7	46.1
OC-SVM	56.9	51.5	50.5	51.8	63.7	50.2	51.2	51.5
IF	50	50	50	50	50.9	50	50.1	50
FB + OCSVM	50.1	53.2	51.8	56.1	62.5	70.5	80.4	89.8
FB + IF	50	50	50	50	54.3	51.3	77.7	67.4
MTL + OCSVM	50	50	50	50	50.2	52.8	54.8	50.7
MTL + IF	50	50	50	50	76.5	75.5	69.3	74.4
OC-MAML (ours)	87.1	86.3	86.8	85.9	92.5	92.4	91.7	92

Table 9: Test accuracies (in %) computed on the class-balanced test sets of the test tasks of the MT-MNIST datasets with $T_{test} = T_{5-8}$. One-class adaptation sets ($c = 0\%$) are used, unless otherwise specified.

Adaptation set size	$K = 2$				$K = 10$			
Model \ Dataset	1	2	3	4	1	2	3	4
FB ($c = 50\%$)	64.6	69.8	68.9	62.9	64.4	83	87.8	72.8
MTL ($c = 50\%$)	60.5	71.4	65	60.6	88.4	91.4	82	79.1
FB	52.2	66.5	54.3	53.8	58.3	63.5	53.6	50.1
MTL	48.5	56.2	51.1	50.1	49.9	51.4	48.5	49.6
OC-SVM	51	53.4	53.9	50.1	50.5	54	54	52.2
IF	50	50	50	50	50	50.2	49.8	50.2
FB + OCSVM	52.2	51.2	50.5	58	86.2	75	84.5	80
FB + IF	50	50	50	50	80.4	87.2	79.2	71.4
MTL + OCSVM	50	50	50	50	51	59.1	71.3	75.9
MTL + IF	50	50	50	50	50	55.7	84.2	64
OC-MAML (ours)	85.9	91.5	85.1	82.5	91.5	95.4	91.4	89.8

Table 10: Test accuracies (in %) computed on the class-balanced test sets of the test tasks of the MT-MNIST datasets with $T_{test} = T_{1-4}$. The results are shown for models without BN (top) and with BN (bottom). One-class adaptation sets ($c = 0\%$) are used, unless otherwise specified.

Adaptation set size	$K = 2$				$K = 10$			
Model \ Dataset	1	2	3	4	1	2	3	4
Reptile	67.1	58.3	57	65.9	82.4	78.5	76.4	81.8
FOMAML	76.3	74.2	74.9	75.6	82.3	75.7	75.1	80.8
MAML	78.1	71.8	77	71.4	88.8	88.7	87.2	86.6
OC-Reptile	50	50	50	50	50	50	50	50
OC-FOMAML	56.6	52.6	55.6	50.1	50.7	50	53.8	64.3
OC-MAML (ours)	85.2	83.5	80.2	84.3	92.5	92.4	91.7	92
Reptile (w. BN)	58.9	56	56.6	62.2	90.4	84.6	88.9	86.7
FOMAML (w. BN)	75.4	72.3	72.2	74.5	91.7	88.6	86	87.8
MAML (w. BN)	83.5	81.3	83.9	77	91.9	90.3	88.7	87.3
OC-Reptile (w. BN)	52	53.2	51.9	51	51.5	51.2	51.1	50.3
OC-FOMAML (w. BN)	74.7	68.5	67	78.7	90.2	85.5	84.3	89.3
OC-MAML (w. BN) (ours)	87.1	86.3	86.8	85.9	92.1	90.7	90.2	91.8

Table 11: Test accuracies (in %) computed on the class-balanced test sets of the test tasks of the MT-MNIST datasets with $T_{test} = T_{5-8}$. The results are shown for models without BN (top) and with BN (bottom). One-class adaptation sets ($c = 0\%$) are used, unless otherwise specified.

Adaptation set size	$K = 2$				$K = 10$			
Model \ Dataset	1	2	3	4	1	2	3	4
Reptile	60.3	65.4	59.9	57.2	73.6	86.3	79.1	72.3
FOMAML	76.5	80.2	77.9	72.8	66.2	84.4	76.9	72.5
MAML	74.8	82.1	73.6	70.7	86.1	93	90.2	85.7
OC-Reptile	50	50	50	50	50	50	50	50
OC-FOMAML	54.6	57.3	59	55	53.3	56.7	51	50
OC-MAML (ours)	80.6	91.5	82.1	77.5	91.5	94.2	91.3	89.8
Reptile (w. BN)	62.3	58.2	60.3	61	85.3	88	88.4	87.2
FOMAML (w. BN)	69.5	75.1	77.3	72.8	86.9	92.3	88.6	85
MAML (w. BN)	84.9	81.8	83.4	76.9	88.6	92.5	90.5	84
OC-Reptile (w. BN)	52	52.2	51.7	53.5	51.1	51.4	50.9	51.8
OC-FOMAML (w. BN)	68.3	85.7	78.5	67.1	83.2	94.7	89.9	82.6
OC-MAML (w. BN) (ours)	85.9	84.8	85.1	82.5	90.5	95.4	91.4	89.8

Table 12: Test accuracies (in %) computed on the class-balanced test sets of the test tasks of the STS-Sine dataset. The results are shown for models without BN (top) and with BN (bottom). One-class adaptation sets ($c = 0\%$) are used, unless otherwise specified.

Model \ Adaptation set size	$K = 2$	$K = 10$
Reptile	52.5	50.0
FOMAML	60.3	52.1
MAML	99.6	99.1
OC-Reptile	50.0	50.0
OC-FOMAML	78.7	58.1
OC-MAML (ours)	99.9	99.9
Reptile (w. BN)	90.9	98.6
FOMAML (w. BN)	90.8	97.3
MAML (w. BN)	51.4	99.0
OC-Reptile (w. BN)	52.6	53.4
OC-FOMAML (w. BN)	78.8	80.0
OC-MAML (w. BN) (ours)	50.5	95.5